EUROPEAN ORGANIZATION FOR NUCLEAR RESEARCH

IS THERE A HIGH-y ANOMALY IN ANTINEUTRINO INTERACTIONS?

M. Holder, J. Knobloch, J. May, H.P. Paar, P. Palazzi, D. Schlatter, J. Steinberger, H. Suter, H. Wahl and E.G.H. Williams
CERN, Geneva, Switzerland

F. Eisele, C. Geweniger, K. Kleinknecht, G. Spahn and H.-J. Willutzki
Institut für Physik*) der Universität, Dortmund, Fed. Rep. Germany

W. Dorth, F. Dydak, V. Hepp, K. Tittel and J. Wotschack
Institut für Hochenergiephysik*) der Universität, Heidelberg, Fed. Rep. Germany

P. Bloch, B. Devaux, M. Grimm, J. Maillard, B. Peyaud, J. Rander, A. Savoy-Navarro and R. Turlay
D.Ph.P.E., CEN-Saclay, France

F.L. Navarria
Istituto di Fisica dell'Università, Bologna, Italy

ABSTRACT

We have analysed data taken in the CERN narrow-band neutrino and antineutrino beams with regard to the "high-y anomaly" observed by preceding experiments at FNAL. At neutrino energies between 30 and 200 GeV, the $\bar{\nu}$ and ν charged-current cross-section ratios and muon-inelasticity distributions disagree with the earlier results. In particular, there is no evidence for energy dependent effects in the antineutrino data which constitute an important aspect of the alleged anomaly.

Geneva - 4 July 1977

(Submitted to Physical Review Letters)

---

*) Supported by Bundesministerium für Forschung und Technologie.

In recent years, low- and high-energy inelastic interactions of neutrinos with nuclei were believed to be consistent with V-A coupling and Bjorken scale invariance in the framework of the spin-$\frac{1}{2}$ parton model[1-4]. In 1974 evidence was reported for a significant departure from expectation of the antineutrino-muon inelasticity distributions at higher energy[5] and subsequently dubbed the "high-y anomaly" after the Bjorken scaling variable $y = (E_\nu - E_\mu)/E_\nu$. Subsequent experimental results supported an anomalous behaviour of $\bar{\nu}$ total and differential cross-sections[6-9]. This was considered as evidence for a deviation from charge-symmetry, together with new particle production[5], the existence of right-handed currents, and a breaking of scale invariance[6]. The experimental observations were the following[10]:

- an excess of events in the high-y region of the antineutrino y-distribution was observed for $x < 0.1$ [5];
- a strong energy dependence of the average value of y was found in the region $E_{\bar{\nu}} = 30\text{-}70$ GeV [6];
- the ratio of antineutrino to neutrino charged-current cross-sections was found to increase with energy above about 30 GeV [7];
- the antiquark component in the antineutrino y-distribution was observed to increase with energy[6,8,9].

We report here first results from an experiment which is currently running at the CERN 400 GeV Proton Synchrotron. The present analysis is addressed to the specific question of a high-y anomaly in antineutrino interactions, and follows, therefore, in part the guide lines set out by the advocates of this anomaly. The experimental conditions, on the other hand, are quite different.

In this experiment, neutrinos and antineutrinos of known energy between 10 and 200 GeV are produced by selecting 200 GeV parents, pions and kaons of the appropriate charge, in 400 GeV proton-beryllium interactions. The parent beam with 0.2 mrad divergence and ±5% momentum spread is directed towards the detector, passing through a 300 m decay tunnel, and about 350 m muon shielding. The average distance from the parent decay point to the detector is 620 m. The beam geometry is well defined apart from the uncertainty in the decay point. This is essential for the determination of the neutrino flux spectrum free from the systematic uncertainties inherent to wide-band neutrino beams. Furthermore, an estimate of the neutrino energy can be obtained event by event from the decay kinematics and the observed radial

distance of a neutrino interaction from the central beam line. The uncertainty in the neutrino energy determined by this means is typically ±20%, mostly due to the unknown decay position along the beam line. Although this measurement of the neutrino energy is not used here in particular, it is useful for a systematic study of the calibration of the detector.

The beam is instrumented by various devices in order to control the alignment, and to measure the beam composition and intensity. Apart from the position detectors, there are, for flux monitoring:

- a differential Čerenkov counter separating pions, kaons and protons;
- a beam current transformer to measure the parent flux;
- a total absorption calorimeter used as beam stopper to integrate the total beam energy;
- a set of detectors in the steel shield to map the ionization generated by the decay muons.

The neutrino energy spectrum and the ratio of neutrino and antineutrino fluxes are accurately known at least for the purpose of the present investigation.

The detector[11] is shown in Fig. 1. Its basic features are the integration of target and detector for both hadron and muon in order to obtain a large acceptance. The muon vector momentum is determined by range or magnetic deflection. The hadronic energy is measured through total absorption calorimetry.

The detector is subdivided into 19 magnetized iron modules, 3.75 m in diameter, with triple-gap drift chambers[12] in between modules for muon track measurement. Each magnet module weighs 65 tons. The average field is 1.65 T giving typically ±10% resolution on the muon momentum. Plastic scintillator is sandwiched with either 5 or 15 cm thick iron plates. There are seven 15 × 5 cm plate modules and twelve 5 × 15 cm plate modules.

The hadron energy is obtained from pulse-height analysis of the scintillator signals. The pulse height is normalized to cosmic ray muons, of which a large sample is taken for this purpose. The response of the calorimeter to hadronic showers was studied separately in a model calorimeter exposed to a pion beam[13]. The results are, in summary, a nearly-linear response with hadron energy, with r.m.s.

resolution of $0.8\sqrt{E*GeV}$ in the 5 cm sampling section of the detector, $\sqrt{3}$ times larger in the 15 cm sampling section. The energy calibration for hadronic showers generated by neutrino interactions has been checked with the help of the known neutrino energy as described above.

The detector is triggered by either a 3 GeV energy deposit in any module, or any three modules with minimum ionizing pulse height, i.e. a 3 GeV muon. In the analysis, further conditions are imposed: a 740 t fiducial volume is defined by cuts in radius and depth, and hits in five consecutive chambers are required on the muon track. The latter requirement ensures a good reconstruction efficiency for muons above 5 GeV momentum. The angular region with good acceptance extends up to 400 mrad typically. This means that the geometric acceptance in y is near unity for all but the upper end of the y-distribution, e.g. $y < 0.9$ for $E_\nu = 100$ GeV.

After fiducial and muon track length cuts there remain 36,000 neutrino and 12,000 antineutrino events. For every event, the neutrino energy is computed from the sum of muon and hadron shower energy, $E_\nu = E_\mu + E_h$. The useful spectrum extends from about 20 to 200 GeV. About half the neutrino data, and a quarter of the antineutrino data, are at energies above 100 GeV. Further cuts are imposed on the data as required for comparison with previous results.

The y-distributions of neutrino and antineutrino events are displayed in Fig. 2 for two different energy bins; in Fig. 3 for all energies $E_\nu > 30$ GeV, with and without a cut at $x < 0.1$. In Fig. 3 the neutrino and antineutrino distributions are normalized to the same neutrino flux in order to allow a test of charge symmetry in the limit $y \to 0$. We note the following: The y-distributions at different energies are very similar. Charge symmetry is valid within our present uncertainties of the neutrino to antineutrino flux ratio (±10%), as is expected for an isospin-zero target when strangeness- and charm-changing currents are neglected. The y-distribution of neutrino events is approximately flat up to $y \simeq 0.9$, where the acceptance losses set in. The antineutrino y-distribution falls rapidly with increasing y as expected for $d\sigma/dxdy \sim q(x)(1-y)^2 + \bar{q}(x)$ in the quark-parton model with a small amount of sea quarks $\int \bar{q}(x)dx << \int q(x)dx$. Even for $x < 0.1$ the y-distributions for neutrinos and antineutrinos are very different, and are compatible with the picture that valence quarks dominate, but that the sea quarks concentrate at small x. These observations are in conflict with Ref. 5 where a flat y-distribution was observed for both neutrinos and antineutrinos in the region $x < 0.1$.

The average values of y for accepted events are displayed in Fig. 4 as a function of neutrino energy. Here a cut $x < 0.6$ has been applied for a direct comparison with Ref. 6. Since the average y-values are biased by the drop in acceptance at large y, we have indicated the expected energy dependence for a constant amount of sea quarks for the conditions of this experiment. The antineutrino data are compatible with an energy independent fraction of sea quarks $B = \int [q(x) - \bar{q}(x)]dx / \int [q(x) + \bar{q}(x)]dx \simeq 0.8$ in contrast to the conclusions obtained in Ref. 6.

From the antineutrino y-distributions, we have calculated the B-values as a function of neutrino energy, and compared them with those of Refs. 6, 8, and 9 (Fig. 5). The new data do not show any significant energy dependence of the quark sea component, contrary to what had been inferred[6,8] from the earlier data.

The ratio of antineutrino and neutrino charged-current cross-sections was computed from the observed number of events, and a Monte Carlo efficiency calculation. The Monte Carlo accounts for the small difference in detection efficiency due to the different y-distributions and the minimum muon momentum required in the analysis. The cross-section ratio is displayed in Fig. 6. We notice that the energy dependence of the antineutrino cross-section follows the neutrino cross-section quite well, in contradiction to the observation of Ref. 7. The present data are subject to two uncertainties: the relative $\bar{\nu}/\nu$ flux normalization has, for the moment, an uncertainty leading to a ±10% scale error common to all energies. In addition, below 90 GeV the events are mostly due to neutrinos from pion decay, and above 90 GeV mostly kaon decay. The ratio of the K/π ratios in the negative and positive beams, as determined using the differential Čerenkov counter, may be in error by not more than ±10%. This could lead to a corresponding discontinuity in the cross-section ratio around 90 GeV, which, however, is not observed.

The present data allow the following conclusions relevant to the "high-y anomaly": the experimental observations on which the evidence was based are not confirmed. In particular, the antineutrino y-distribution, and the ratio of antineutrino-to-neutrino cross-sections, are found to be essentially independent of neutrino energy. There is no high-y anomaly.

REFERENCES AND FOOTNOTES

1) T. Eichten et al., Phys. Letters 46B, 274 (1973).

2) A. Benvenuti et al., Phys. Rev. Letters 30, 1084 (1973).

3) B.C. Barish et al., Phys. Rev. Letters 31, 656 (1973).

4) H. Deden et al., Nuclear Phys. B85, 269 (1975).

5) B. Aubert et al., Phys. Rev. Letters 33, 984 (1974).

6) A. Benvenuti et al., Phys. Rev. Letters 36, 1478 (1976).

7) A. Benvenuti et al., Phys. Rev. Letters 37, 189 (1976).

8) B.C. Barish et al., Phys. Rev. Letters 38, 314 (1977).

9) J.B. Berge et al., "Scaling variable distributions for antineutrino-nucleon interactions", preprint FERMILAB-Pub-77/44-Exp, (1977), submitted to Phys. Rev. Letters.

10) The scaling variables are defined as $x = Q^2/2M_\nu$ and $y = \nu/E_\nu$ where Q^2 is the square of the four-momentum transfer from the neutrino to the muon, and ν is the energy transfer to the hadrons.

11) M. Holder et al., "A detector for high-energy neutrino interactions", submitted to Nuclear. Instrum. Methods.

12) G. Marel et al., Nuclear Instrum. Methods 141, 43 (1977).

13) M. Holder et al., "Calibration of a magnetized total absorption calorimeter", submitted to Nuclear Instrum. Methods.

Figure captions

Fig. 1 : Side view of the detector. The neutrino beam enters from the left.

Fig. 2 : The y-distributions of neutrino and antineutrino events with $x < 0.6$ in the two energy bands E_ν = 30-40 GeV and E_ν = 100-150 GeV, respectively.

Fig. 3 : Normalized y-distributions for neutrino and antineutrino data, with and without a cut $x < 0.1$. The distributions are normalized to the same ν and $\bar{\nu}$ fluxes subject to a relative scale error of ±10%.

Fig. 4 : The first moments of the y-distributions as a function of energy, for neutrino and antineutrino data with $x < 0.6$. The curves marked B = 0.8 are calculated for the conditions of this experiment assuming a fixed antiquark component. The HPWF data are taken from Ref. 6.

Fig. 5 : The B-values as a function of antineutrino energy, from various experiments (Refs. 4, 6, 8, and 9).

Fig. 6 : The ratio of antineutrino-to-neutrino charged-current total cross-sections as a function of neutrino energy. The data marked HPWF1/2 are taken from Ref. 7. The indicated errors are statistical only. Systematic errors are discussed in the text.

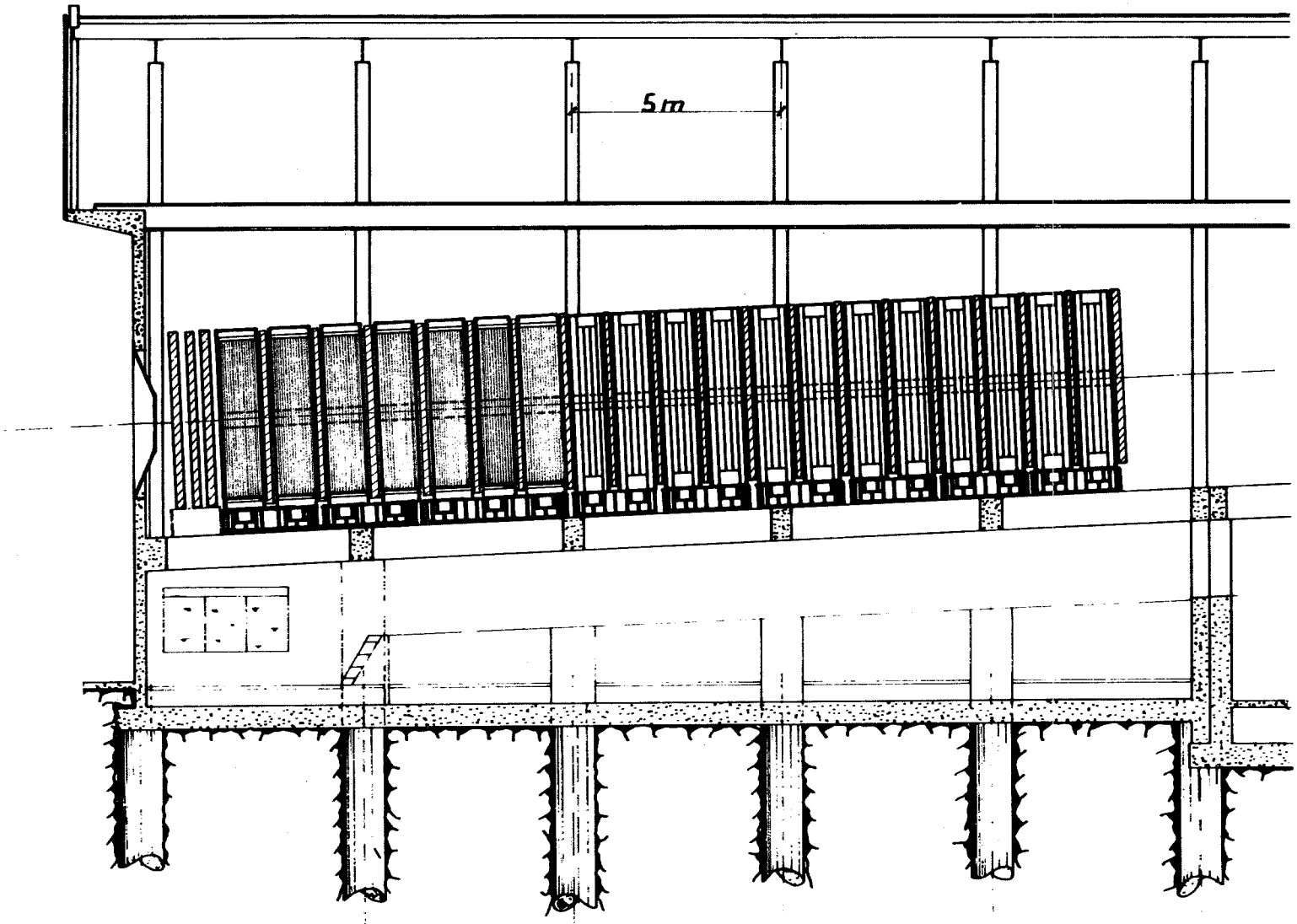

Fig. 1

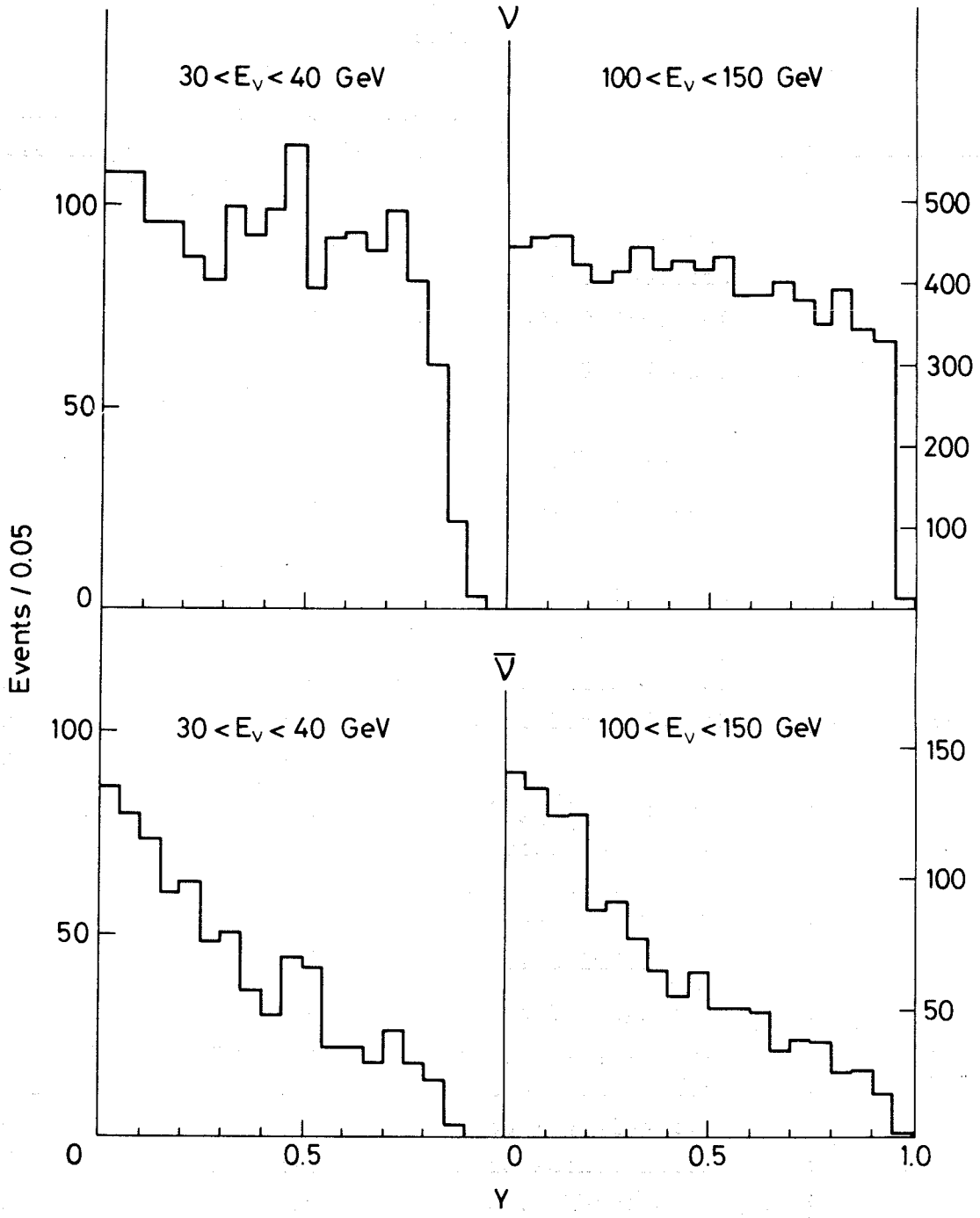
ν
30 < Eν < 40 GeV
100 < Eν < 150 GeV
100
50
0
500
400
300
200
100
Events / 0.05
ν̄
30 < Eν < 40 GeV
100 < Eν < 150 GeV
100
50
0
150
100
50
0
0.5
0
0.5
1.0
Y

Fig. 2

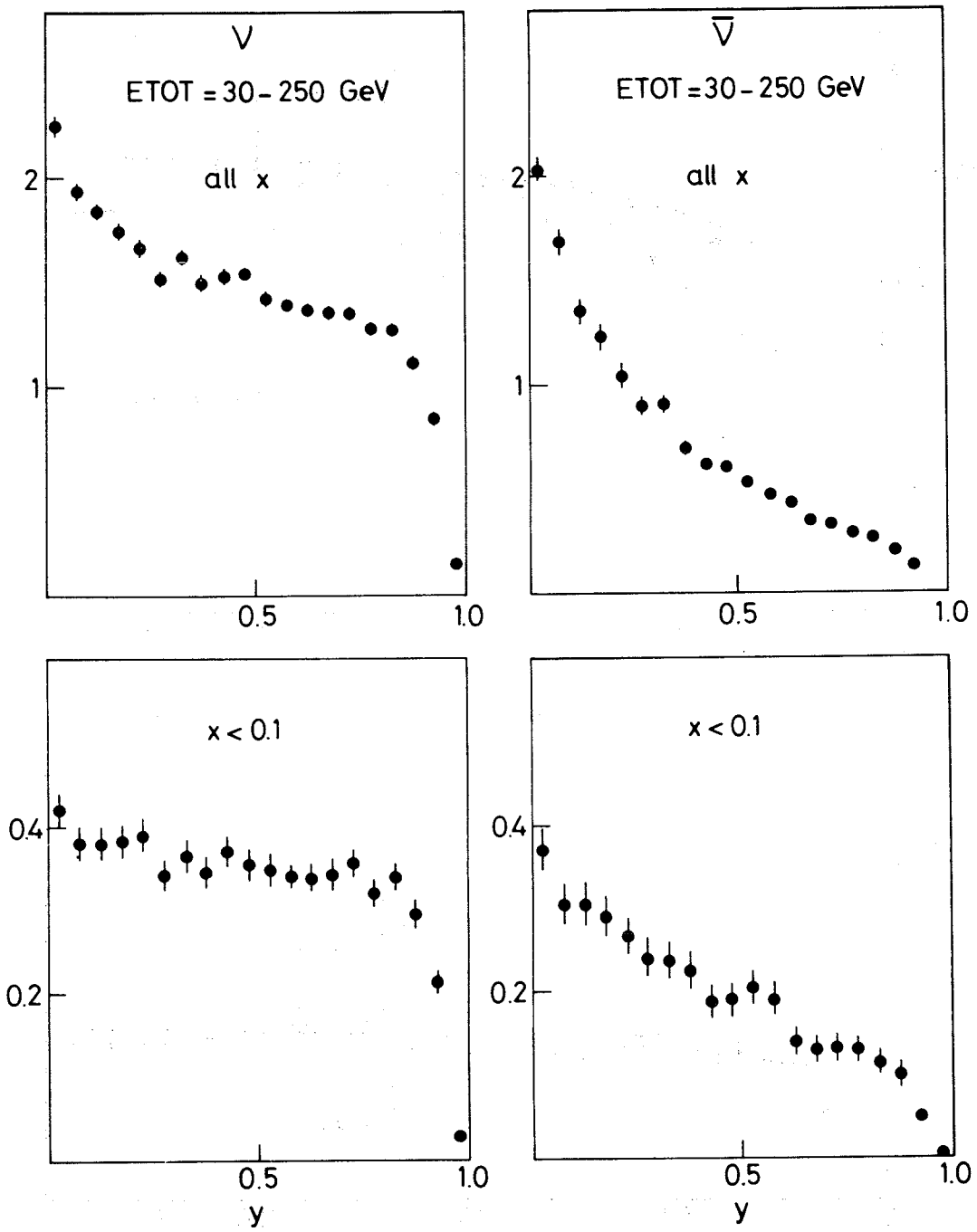
ν
ETOT = 30 - 250 GeV
all x
2
1
0.5
1.0
$\bar{\nu}$
ETOT = 30 - 250 GeV
all x
2
1
0.5
1.0
x < 0.1
0.4
0.2
0.5
1.0
y
x < 0.1
0.4
0.2
0.5
1.0
y

Fig. 3

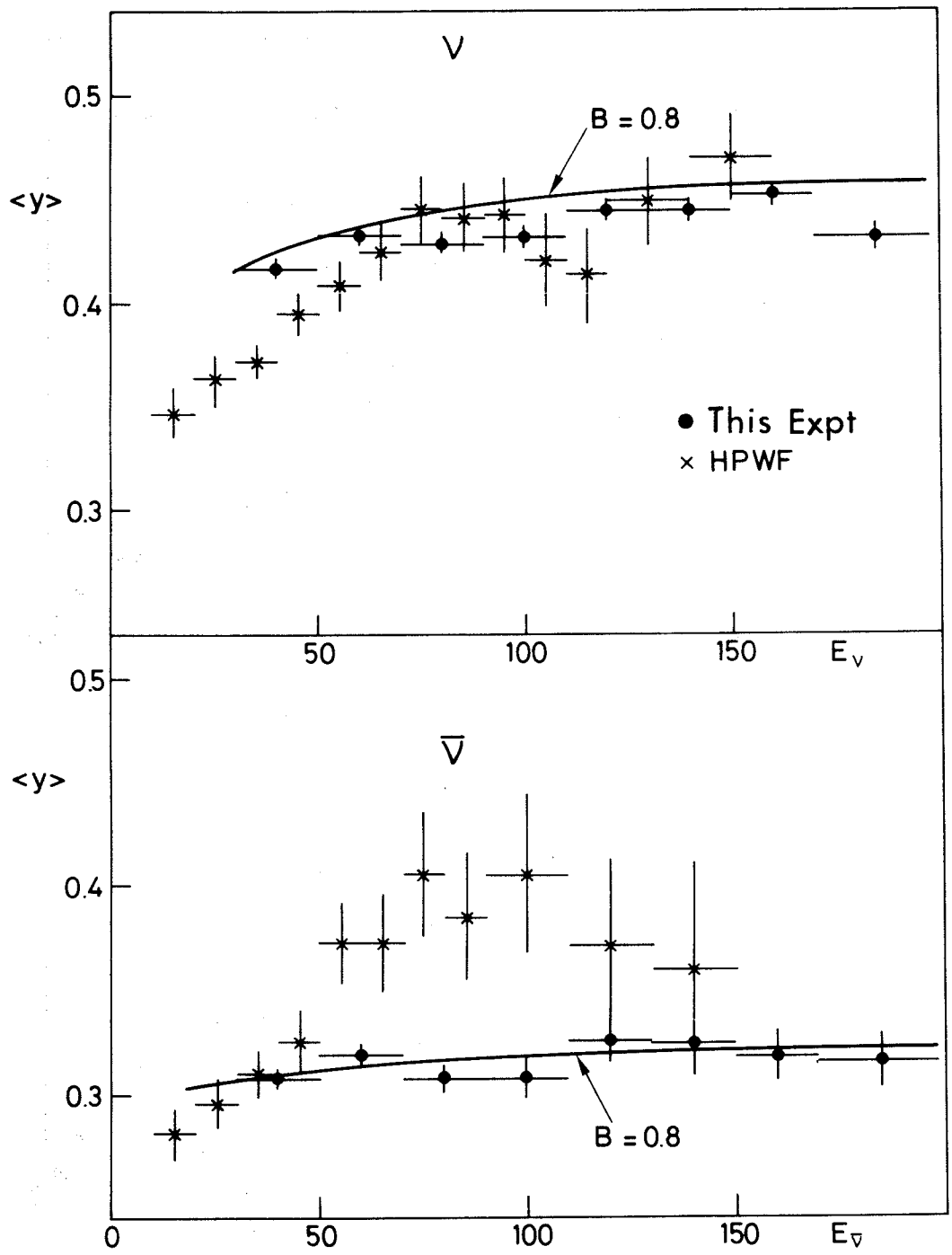

Fig. 4

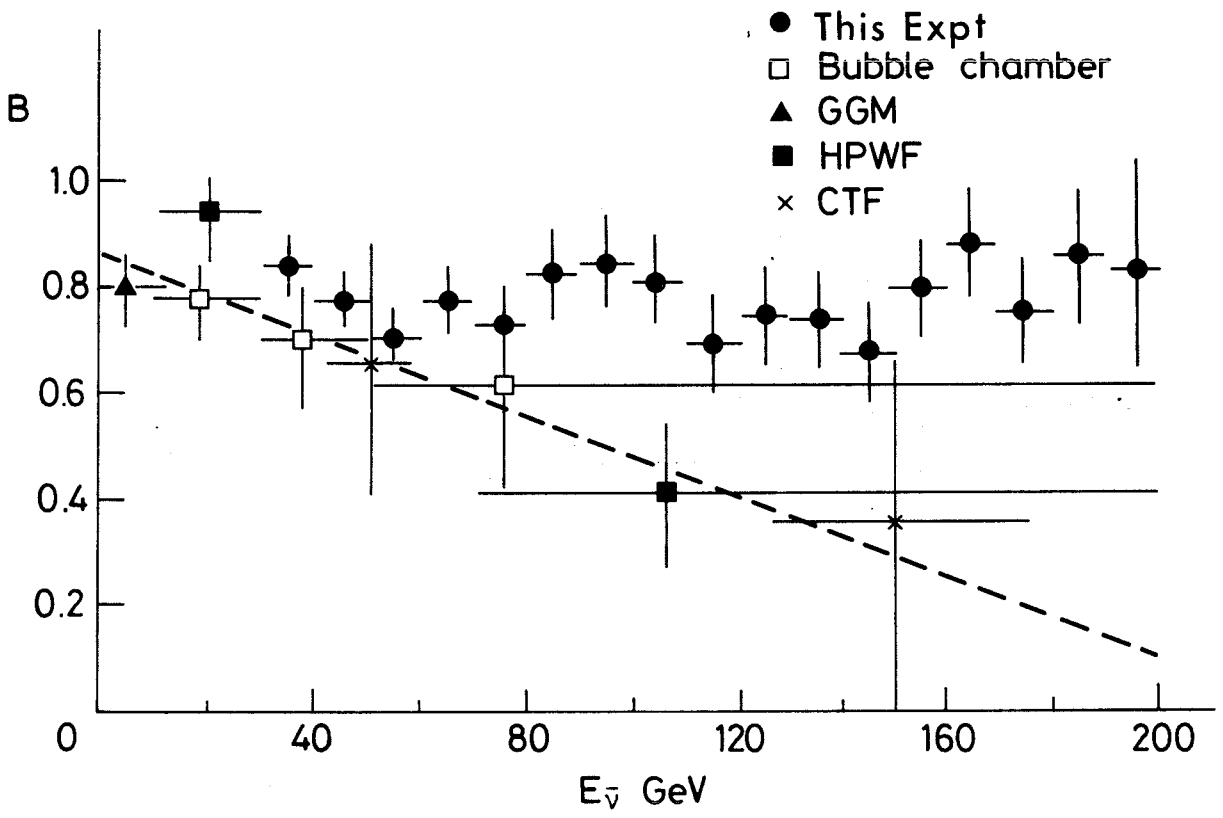
This Expt
Bubble chamber
GGM
HPWF
CTF
B
1.0
0.8
0.6
0.4
0.2
0
40
80
120
160
200
$E_{\bar{\nu}}$ GeV

Fig. 5

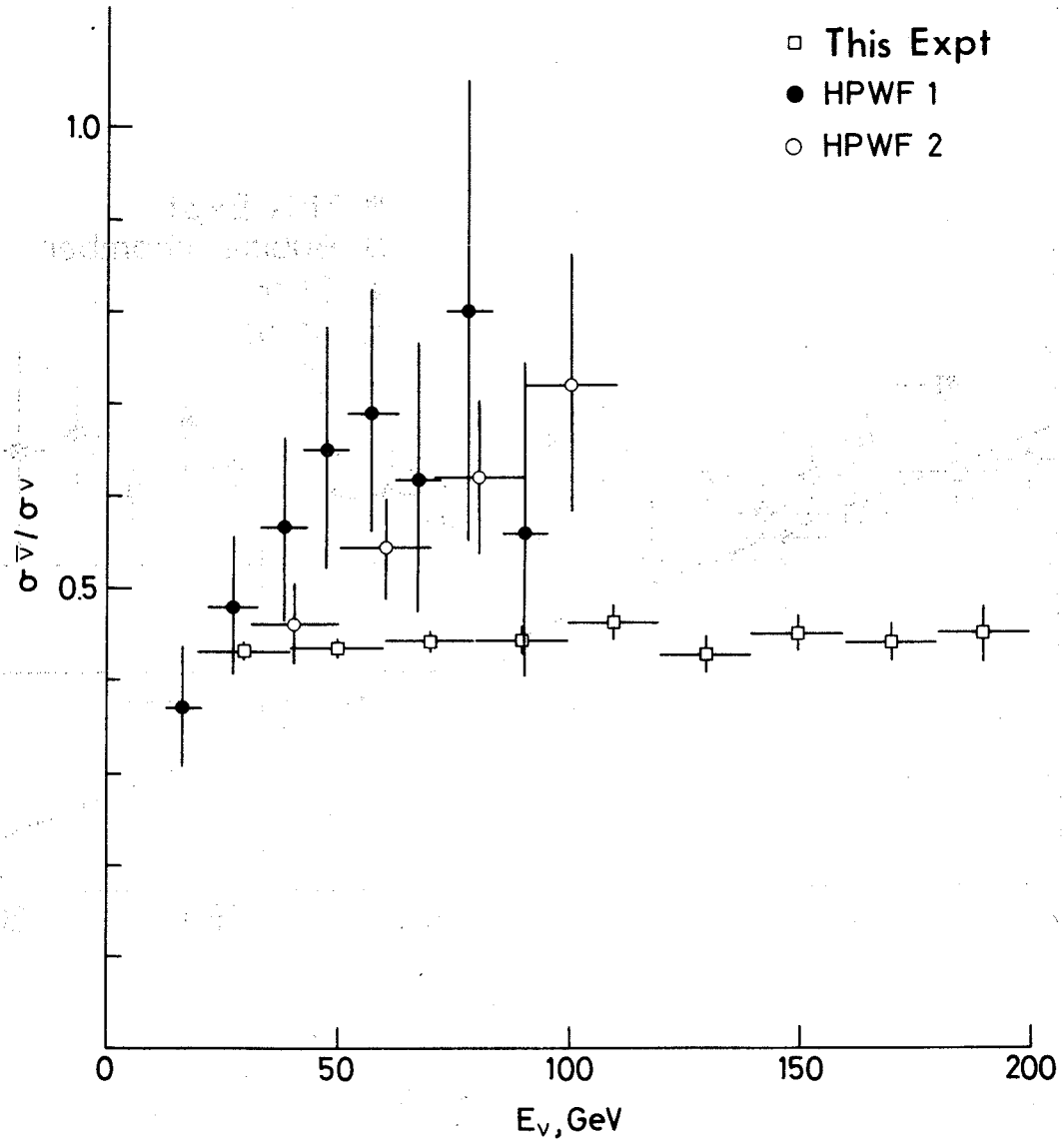
This Expt
HPWF 1
HPWF 2
1.0
0.5
$\sigma_{\bar{\nu}}/\sigma_{\nu}$
0
50
100
150
200
E_ν, GeV

Fig. 6